Study of θ_1^0 Production and Decay by Observation of Its Neutral Decay Mode*

JOHN E. OSHER,† BURTON J. MOYER, AND SHERWOOD I. PARKER
Department of Physics and Radiation Laboratory, University of California, Berkeley, California
(Received November 25, 1958)

The production of strange particles possessing neutral-pion decay products has been investigated in proton bombardment of Bevatron targets. A well-collimated telescope counted energetic gamma photons originating within a few centimeters of the target. The position-dependent counting rate was determined by moving the telescope and collimation on a track parallel to the beam direction, and the resulting data were then compared to curves calculated from certain assumed kinematical models consistent with associated production. The counting rate and its variation with position were consistent with the identification of $\theta_1^0 \to 2\pi^0$, which implies even spin and even parity. The data also allow some gamma-ray contributions from $\theta^+ \to \pi^+ + \pi^0$, $\Sigma^+ \to p + \pi^0$, and $\Lambda^0 \to n + \pi^0$. The ratio of intensities from regions "upstream" to those "downstream" from the target implies a strongly peaked angular distribution, forward and backward, in the reference frame of the colliding nucleons which produce the θ_1^0.

I. INTRODUCTION

THE study of the very-short-lived ($\sim 10^{-10}$ sec) species of strange particles requires that observations must be made at distances within a few centimeters from the point of production. In the case of production by proton bombardment, and in the absence of a proton beam emerging externally from the accelerator, it is necessary to devise means of identifying the particles in question as they decay in the immediate vicinity of the Bevatron target.

For those strange particles whose decay products include neutral pions, which in turn decay within $<10^{-15}$ second predominantly into energetic photons, it is possible to identify their production and decay by means of a rigidly-collimated telescope for high-energy photons, so oriented as to receive photons only from a selected, limited region of space near the target. The $K_{\pi 2}$ and the Σ^+ were known to yield π^0 decay particles; at the time of the inception of this experiment it was not known whether or not both the K^0 and the Λ^0 had neutral decay modes.

Such a technique is similar to the early attempts at measuring π^0 lifetime by Bjorklund *et al.*,[1] to the unsuccessful search for strange-particle production at lower proton energies by Garwin,[2] and by Balandin *et al.*,[3] and to the successful strange-particle work of Ridgway, Berley, and Collins[4] at the Brookhaven cosmotron. In the present experiment the counter telescope and its associated collimation were oriented at 90° (laboratory angle) from the direction of the Bevatron beam at the target, and the whole system was translated upstream and downstream from the target in order to observe the projected decay density of the strange particles as a function of distance from the target in these directions.

These data were then analyzed by a best-fit comparison to calculated decay curves for various possible kinematic combinations.

In formulating the kinematics, use was made of available experimental data as to the expected production mechanisms and decay characteristics. In particular, associated production of the form $p+N \to N+Y+K$ was assumed, consistent with Gell-Mann's theory.[5] The work of Ridgway *et al.*[4] at Brookhaven in an experiment very similar to the one discussed here has demonstrated that the production threshold agrees with this production model.

Other reactions undoubtedly do contribute, including production through intermediate pion states and four-body final states, but these other forms were assumed to be of minor consequence for production from protons in the energy range of 2.0 to 6.2 Bev. Recent data seem to imply that $p+p \not\to K^0+Y^+ +p$, but indicate reasonable production from $p+n \to K^0+Y+N$.[6] The kinematic details for all of the known strange particles capable of π^0 modes of decay were calculated under selected assumptions about their production, using the decay mechansim, established Q values, and ranges of lifetime as determined from other experiments. The best fit to the data obtained is discussed in Sec. V below, together with the specific assumptions made and the kinematical features involved.

The results will be seen to affirm the neutral decay mode of the θ_1^0 meson and to allow an estimate of the fraction of its decays via this mode. Also some inferences concerning the angular distribution of the θ_1^0 production can be made for reactions of the type here involved.

* This work was done under the auspices of the U. S. Atomic Energy Commission.
† Now with Los Alamos Scientific Laboratory, Los Alamos, New Mexico.
[1] Bjorklund, Crandall, Moyer, and York, Phys. Rev. **77**, 213 (1950).
[2] R. L. Garwin, Phys. Rev. **90**, 274 (1953).
[3] Balandin, Balashov, Zhukov, Pontecorvo, and Selivanov, J. Exptl. Theoret. Phys. U.S.S.R. **29**, 265 (1955) [translation: Soviet Phys. JETP **2**, 98 (1956)].
[4] Ridgway, Berley, and Collins, Phys. Rev. **104**, 513 (1956).
[5] M. Gell-Mann and A. Pais, *Proceedings of 1954 Glasgow Conference on Nuclear and Meson Physics* (Pergamon Press, London, 1955), p. 342.
[6] D. Berley and G. B. Collins, Bull. Am. Phys. Soc. Ser. II, **1**, 320 (1956).

II. EXPERIMENTAL ARRANGEMENT AND PROCEDURES

A. Disposition of Apparatus and Bevatron Facilities

The counter telescope and collimation assembly (shown in Fig. 1) were mounted as a rigid unit which could be moved along on tracks located over a vertical re-entrant "well", possessing a Lucite bottom window, at the west tangent tank of the Bevatron. The location in regard to the Bevatron is shown in Fig. 2. This location allowed the collimation assembly to extend within 10 inches of the target and yet permitted the counter telescope and collimation assembly to be moved by remote control so as to view regions as much as 15 cm either upstream or downstream from the target.

The energy of the proton beam was determined from the magnetic-field strength which was monitored by a system of magnet-current markers. The beam was spilled onto the target for a time interval of nearly 100 milliseconds to reduce the instantaneous counting rates for the electronics. This prolonged spill, and the change of magnetic field with time, of course resulted in an energy spread in the proton beam. The target was plunged to the proper location under the counter assembly after the large initial beam oscillations had damped out; also a clipper was simultaneously plunged at a location 180° around the machine to remove the protons which had gained large radial oscillations from scattering by passage through the target, and to prevent them from hitting the target holder and target plunging probe.

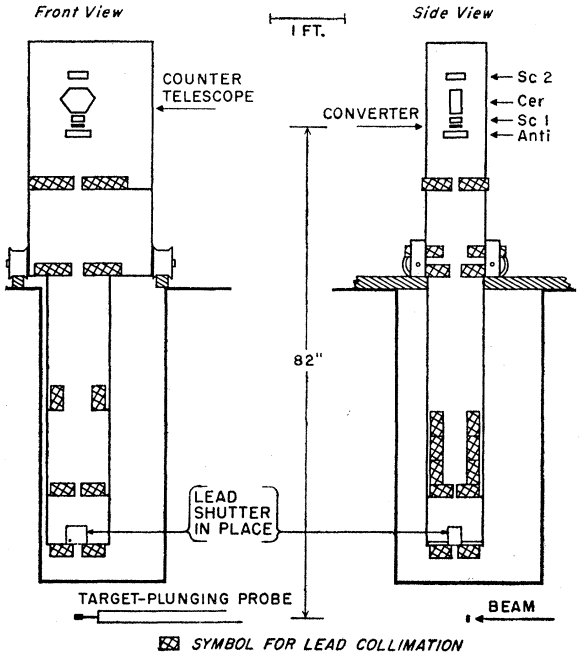

FIG. 1. Front and side cross sections of the counter telescope, collimation, and mounting system.

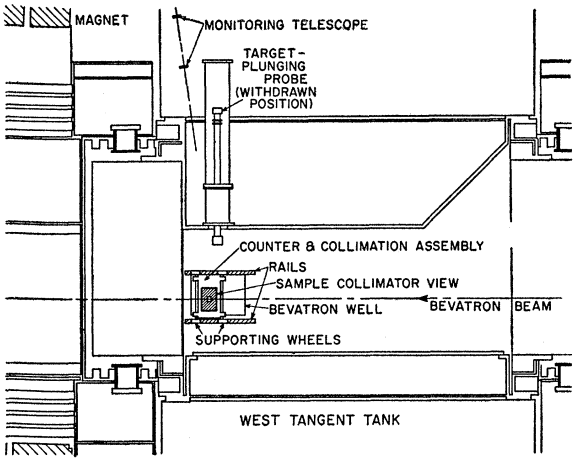

FIG. 2. Vertical view down on Bevatron west target area. Location of Bevatron "well," counter system, and monitoring telescope are shown.

B. Counter Telescope and Calibration

The telescope-counter array is shown in Fig. 1. The sequence of events for a detected gamma photon would be (a) no pulse from the front plastic scintillator (anti), (b) conversion of the photon in the lead converter, (c) a pulse resulting from the passage of at least one charged particle through the plastic scintillation counter SC1, (d) a pulse in each of the Čerenkov-counter phototubes from at least one relativistic particle passing through the 10-cm Lucite Čerenkov counter, and finally (e) a pulse from a charged particle entering the rear counter SC2. The Pb converter was constructed so that it could be placed at standard "in" or "out" positions by remote control.

Since the counter was to operate in a strong pulsing magnetic field, extensive magnetic shielding was used. The magnetic shielding of the phototubes was checked by monitoring the counting rate for each of the phototubes during the Bevatron magnetic cycle (using no beam), with an insert of a plastic scintillator on the Čerenkov counter, and with a radioactive source placed near the scintillators.

A block diagram of the counter array and associated electronics is shown in Fig. 3. The electronics used had a resolving time of approximately 10^{-8} sec, being limited primarily by the anticoincidence circuit. The very flexible multiple-coincidence circuit and anticoincidence circuit used is of standard Radiation Laboratory design.[7]

The counter telescope was calibrated by a combination of experimental and theoretical methods.[8,9] The procedure was to determine experimentally the electron-

[7] M. Nakamura, University of California Radiation Laboratory Report UCRL-3307, 1956 (unpublished).
[8] J. E. Osher, University of California Radiation Laboratory Report UCRL-3449, June, 1956 (unpublished).
[9] R. K. Squire, University of California Radiation Laboratory Report UCRL-3137, September, 1955 (unpublished).

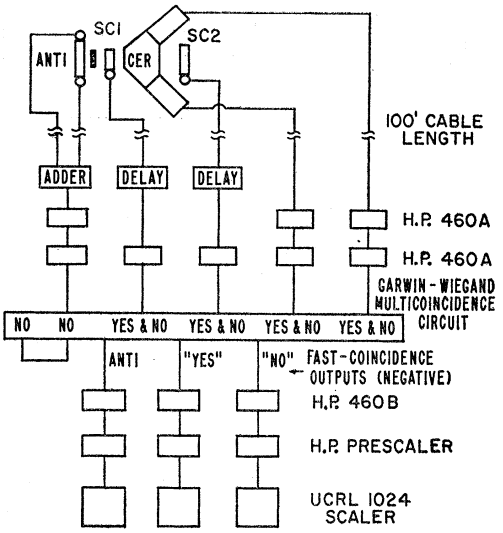

FIG. 3. Electronics and counter block diagram.

counting efficiency of the counter telescope (without its front "anti" counter or regular lead converter) as a function of Pb-foil thickness (varied from 0 in. to $\frac{1}{4}$ in.) in the converter position, as a function of incident-electron energy (experimentally varied over the range 40–300 Mev), and for various geometrical positions of normal incidence upon the Pb foil. This is in effect the simulation of a gamma conversion at a known position and depth in the converter into an electron of known energy. This electron efficiency was then extrapolated (in an asymptotic region of the curve) to include electron energies of 300–700 Mev and folded with the theoretical probabilities of pair formation in the various increments of distance through the actual lead converter, and with the theoretical energy-partition probabilities for the electron and positron. In the experiment the 340-Mev synchrotron was used as the source of electrons by directing the bremsstrahlung beam on a converter placed at the entrance of a pair magnet to yield a spectrum of electrons. The electron energy was determined by a calibrated momentum channel in the pair magnet. And finally an electron telescope of small dimensions was added in front of the counter telescope to define further the momentum channel, to count the incident electrons, and to define the position of incidence. The ratio of the number of incident electrons giving a simultaneous counter telescope pulse to the total number of incident electrons then is by definition the electron-counting efficiency of the counter telescope. The resulting gamma-counter efficiency for our geometry as determined by this method is shown in Fig. 4 with about $\pm 15\%$ accumulated absolute error.

C. Collimation

The collimation assembly as shown in Fig. 1 was found necessary in order for the counter telescope to observe gammas originating in regions of space near the target without an extensive background from the target, which represented an extremely intense source of gammas because of direct π^0 production. Even with the large amount of lead employed, a relatively small background was present and had to be subtracted from the data. The corrections for effects of direct π^0 production in the target and for target gammas scattered from the collimation slits are given in Sec. III. The efficacy of the collimation may be judged from Fig. 5, obtained under conditions producing only target π^0's.

D. Monitor and Calibration

The relative monitor used in this experiment consisted of a pion telescope (two 1-in. diam, $\frac{1}{2}$-in. thick plastic scintillators—as shown in Fig. 2). This relative monitor was chosen because it gave an accurate instantaneous record of the proton flux through the target, as it looked essentially at the charged-pion production occurring in the target. The induction-

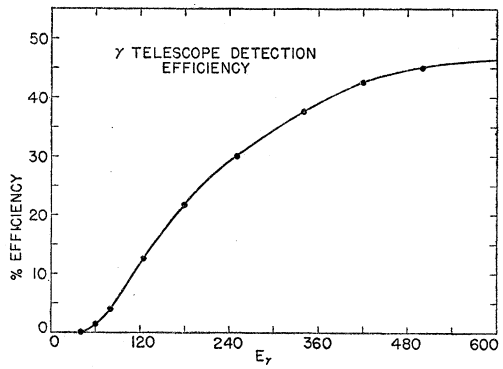

FIG. 4. Gamma-counter telescope detection efficiency as a function of gamma energy for collimated gamma radiation incident on the counter telescope.

electrode signal was used as a rough preliminary calibration of the circulating beam, but for final analysis the pion telescope was calibrated by plunging thin aluminum foils with the target. An absolute calibration was made by correlating the monitor counts against the Na^{24} activity[10] (a spallation product from Al) produced in 2-hour runs with an aluminum sandwich (1-mil guard foil, 2-mil Al, 1-mil Al guard foil) covering the target face. This then took proper account of multiple traversals through the target, and of beam missing the target, which are the sources of error in the circulating-beam induction-electrode measurement. This method, on the other hand, introduces an appreciable error (at least $\pm 20\%$) in the absolute production cross sections given in Sec. V, pending a better value of the Al-spallation cross section to form Na^{24} (taken here as 9.3 mb for 6.0-Bev protons) and a better correction for the production of Na^{24} by neutrons which are them-

[10] Friedlander, Hudis, and Wolfgang, Phys. Rev. 99, 263 (1955).

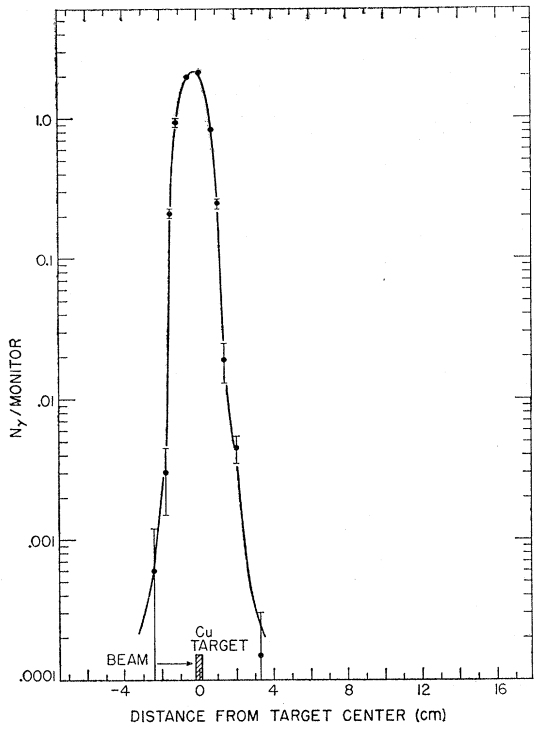

FIG. 5. Data taken at 0.8 to 1.0 Bev, below associated production threshold, to determine the effective slit resolution for a specific target thickness, slit width $\frac{1}{2}$ inch.

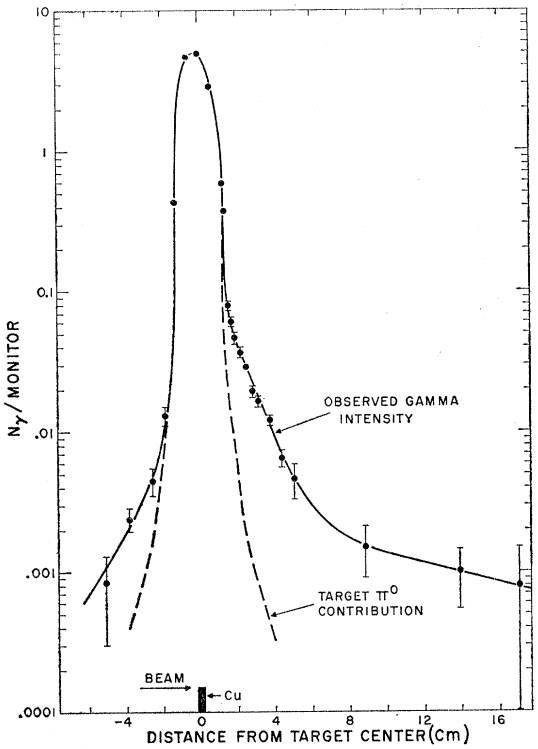

FIG. 6. Data for 5.7- to 6.0-Bev protons incident on a $\frac{1}{8}$-in. Cu target, observed with $\frac{1}{2}\times 1$-in. slits for the lower defining aperture.

selves produced in the target (here estimated as a 15% correction for the $\frac{1}{2}$-in. Cu target).

III. TREATMENT OF DATA

The numbers plotted in the curves presented below represent the counting rates for high-energy photons received from various locations of the column of space defined by the collimating system. These numbers are the result of a combination of four observed counting rates measured under the following conditions:

(a) Pb converter in, channel open (i.e., Pb shutter removed; see Fig. 1);
(b) converter out, channel open;
(c) converter in, channel closed;
(d) converter out, channel closed.

The difference between (a) and (b) is related to electrons originating in the converter when the channel is open; the difference between (c) and (d) gives a small background counting rate for electrons originating in the converter but not attributable to gamma rays from the volume of space of interest. This background, due presumably to events generated by neutrons and charged pions in the material of the collimating system and converter, was fortunately a small, nearly constant correction to be subtracted from the (a) minus (b) data. It was important only at the extreme upstream and downstream limits of the data displayed.

The counting rate as observed above might be expected to include some gammas from direct π^0 production in the target directed by slit scattering into the counter aperture. Consequently the collimating function was directly measured to determine the spatial resolution and enable the direct π^0 production to be subtracted away. This measurement was performed by reducing the beam energy to 0.8 to 1.0 Bev (below associated production threshold) and making a spatial determination of the apparent target size as viewed from direct π^0 gammas. This experimental slit-scattering measurement was applied for other energies simply by normalizing to the same on-target gamma intensity, because the behavior of high-energy gammas was not expected to change in any essential way, even though a slight change of gamma spectrum could be expected at 90° (laboratory) with a change in Bevatron energy. The resolution curve from a $\frac{1}{8}$-in. Cu target is shown in Fig. 5; this was cross-checked on the upstream side for proton energies below 3 Bev (kinematically K mesons could not go upstream for proton energies below approximately 3 Bev).

Experimental data obtained as thus described are given in Fig. 6 for which the target thickness was $\frac{1}{8}$ in. (Cu) and the lower defining aperture of the collimating system was $\frac{1}{2}\times 1$ in. The $\frac{1}{2}$-in. dimension is measured parallel to the $\frac{1}{8}$-in. target-thickness dimension, i.e., parallel to the beam direction. This lower defining

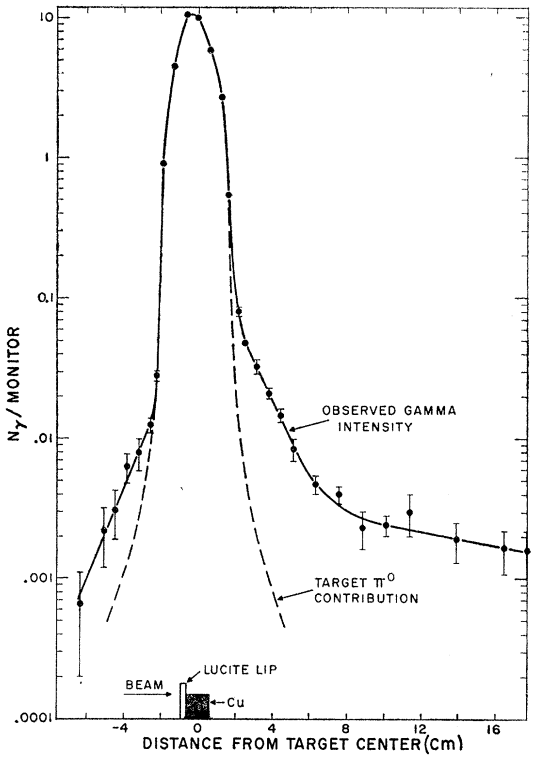

FIG. 7. Data for 5.7- to 6.2-Bev protons incident on a $\frac{1}{2}$-in. Cu target, observed with $\frac{1}{2}\times 1$-in. slits for lower defining aperture.

aperture is not the lowest aperture shown in Fig. 1, but is the second aperture encountered in proceeding upward from the target region. The lowest, broader aperture is simply a passage through a Pb structure which shields the defining aperture from direct irradiation from the target. The edges of this lowest aperture do not "see" the counter telescope. The transverse dimension (here 1-in.) of the defining aperture substantially affects the observed slope of the curves of intensity *vs* distance, owing to loss of the diverging particles; but this effect is, of course, calculable if an angular distribution is known or assumed.

Similarly, in Fig. 7 are shown the data from a $\frac{1}{2}$-in. Cu target obtained with the same collimation as described above. In both Figs. 6 and 7, the dashed curves represent the normalized contribution of direct target π^0's and the slit scattering of their photons. Figure 8 presents the results of observations for four different energy intervals of the incident protons, in which the direct π^0 contribution has been subtracted away. In Fig. 10 are plotted the counting rates at a fixed position 2.5 cm downstream from the target for the various energies involved in the data of Fig. 8.

IV. QUALITATIVE DISCUSSION OF RESULTS

Before entering into a discussion of the kinematical assumptions and calculations, and of certain trial functional forms for the matrix element describing the production of the particles whose decays are observed, we shall summarize the qualitative features of the data which are of interest and which must be accommodated by the assumptions and calculations.

A. The Gamma Rays Originating "Upstream"

The presence of observed photons, definitely in excess of those due to slit scattering of target π^0 photons, when the volume region selected by the collimator was upstream from the target, requires that the most prominent particles in question be of mass comparable to K mesons rather than to hyperons. The latter particles could not emerge upstream in the laboratory from energies here available in the nucleon-nucleon collision systems, except by scattering; and it would be extremely difficult to explain the observed upstream intensity and spatial decay rate upon this basis. Figures 6, 7, 8, and 9 all exhibit the upstream component clearly for those cases in which the incident-beam proton energy was well over 3.0 Bev. When the beam energy was below about 3.0 Bev this component was not present, which is kinematically appropriate for particles of K-meson mass.

Furthermore, the ratio of the intensity of upstream emission to that of downstream emission, together with the spatial-decay slope of the former, has led us to postulate a strongly peaked, forward and backward contribution in the production of θ^0's in the reference frame of the colliding nucleons.

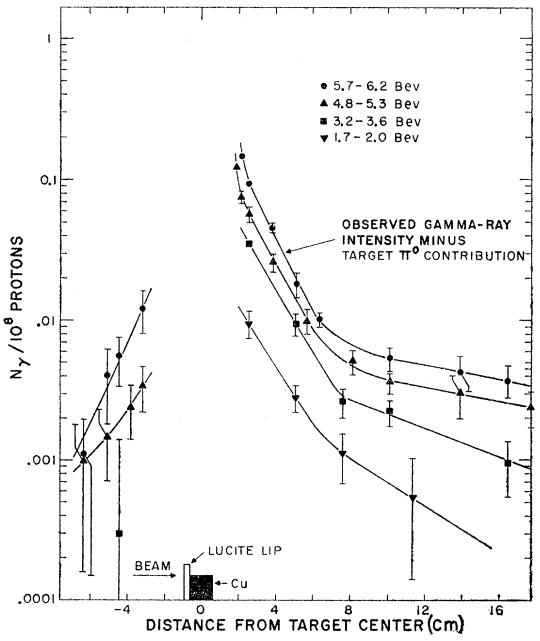

FIG. 8. Data for the proton energies listed above incident on a $\frac{1}{2}$-in. Cu target, as observed with a $\frac{1}{2}\times 1$-in. slit as lower defining aperture.

B. The Rate of Variation of Intensity with Position

The spatial-decay slopes observed in the plots of photon intensity *vs* position of collimator are compatible with particle lifetimes of the order of 10^{-10} second. It is impossible to completely identify the separate contributions of the π^0-decay modes of the Σ^+, Λ^0, K^+, and θ^0 particles; but there are reasons related to the spectral efficiency of the counter telescope, and to kinematics (which will be discussed below in Sec. VB), for believing that the observed photons are predominantly from the θ^0 particles.

Furthermore, it is possible to understand the ratio of upstream to downstream intensities, as well as the decay slopes of both, in terms of the θ^0's; but it is difficult to accommodate these observations if the hyperons are prominently seen by the counters.

In the downstream intensity variation a change of slope is evident at a distance of several centimeters from the target. This can be produced by the effects of the peaked angular distribution assumed for a part of the θ^0 yield, and it also is related to the contribution of the K^+ mesons and to a slight extent of the Λ^0's.

It has been previously mentioned that the apparent initial decay slopes are strongly affected by the angular distribution because the loss of particles from the field of view as the collimator is translated away from the target is a function of their angular distributions.

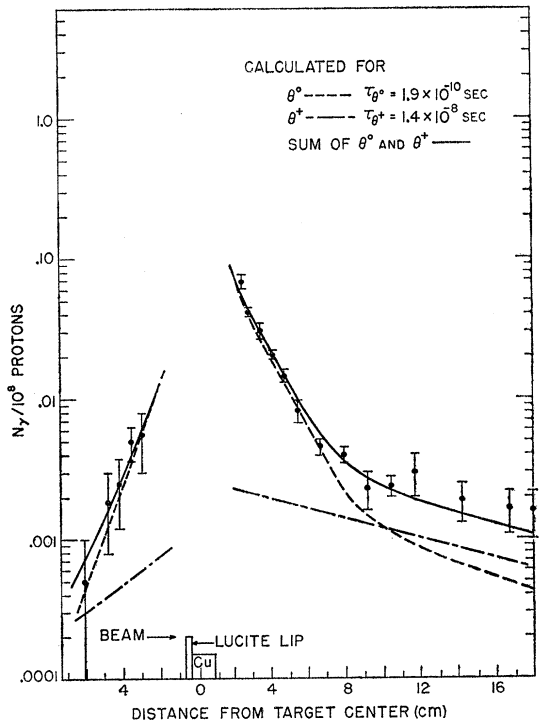

FIG. 9. Calculated curves for θ decay and θ^+ decay compared with the experimental data of Fig. 7. The θ^0 and θ^+ curves were calculated for equal cross sections, and matrix-element energy and angular dependencies of $|H|^2 \propto \{E^2/M^2-1\}\cos^{14}\theta$ in the c.m. system, where E, M, θ refer to the particular particle in question.

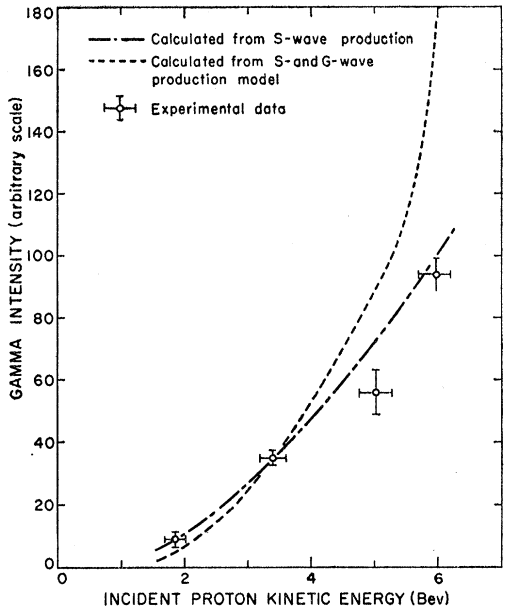

FIG. 10. Excitation function of gamma intensity *vs* energy at fixed distance of 2.5 cm from target center.

C. Magnitude of the Yield

Since the counter telescope efficiency is determined upon an absolute basis, and since the geometric definition of the volume of space contributing detectable photons is known, it is possible to estimate the absolute production cross section for the short-lived particles observed via the two-π^0 decay if angular and momentum distributions are assumed.

For the examples of angular and momentum distributions described below in Sec. V, the absolute-production cross sections, per target nucleon, for creation of particles seen through an assumed decay into two π^0's, were in the range of 0.2 to 0.5 mb. While this was but a crude result, it was evidence for a substantial fraction of the θ_1^0 decay proceeding via the neutral mode. Further work with counters to measure the ratio of charged-pion to neutral-pion decay modes is being pursued.

D. Excitation Function

The dependence of photon yield (measured 2.5 cm downstream from the target) upon bombarding proton energy is shown in Fig. 10. This also is an empirical result to be satisfied by the momentum dependence assumed in the trial matrix elements.

V. KINEMATICS AND MATRIX ELEMENTS

A. Kinematical Assumptions

For the purposes of calculating phase-space factors and energy distributions, the major contribution of

strange particles here observed was assumed to be from the 3-body, final-state type, $N+N \rightarrow N+Y+K$. The calculational procedure then involved the following items:

(a) The energy distribution of protons incident upon the target was ascertained from the operational characteristics of the Bevatron. For example, under conditions of highest energy, the prolonged beam "spill" on the target required for satisfactory counter operation involved a nearly uniform spread in incident-proton energy from 5.7 to 6.2 Bev.

(b) The momentum distribution of the target nucleons was assumed to be of the Fermi type with a 24-Mev upper limit. This, together with (a), determines the distribution in available energies in the reference frames of the colliding nucleons, and also determines the laboratory velocity distribution of the collision systems. Calculations were also made with a Gaussian-type momentum-density function, with results which differed only slightly due to the "tail" of high momenta. For incident-proton energies above 3 Bev, the results of the two distributions are essentially indistinguishable.

(c) A 3-body, relativistic phase-space calculation, conserving total energy and momentum in the collision reference frame, provided the velocity spectrum within that frame of any desired particle in the final state.[11] No attempt was made to conserve angular momentum in the calculations. Probably many angular momenta contribute, though the analysis given below of matrix elements will indicate that high angular-momentum states may be prominent contributors.

(d) An energy- and angular-dependence function is now assumed as a matrix element effective in the production of the K mesons, the parameters of which are to be adjusted for an empirical fit to the data. We are now able to calculate the spatial and velocity distribution of the K mesons in the reference frame of the production collision.

(e) It is assumed, consistent with zero spin, that the K-meson decay is isotropic in its own reference frame. Furthermore, the decay of a π^0 meson is isotropic in its own frame. Consequently the photon distribution from this process will be spherically symmetric in the rest frame of the K meson, and will possess a spectrum in this frame which is flat between a minimum and maximum value of photon energy which are readily determined by the Doppler shift due to π^0 motion within the K-meson frame.

(f) The volume of space defined in the laboratory reference system by the collimation is now used to define by transformation the limitations in the collision reference frame within which the π^0 decay of a K meson can be counted. It is then possible to calculate the probability that a K meson of a particular momentum, and within an eligible solid angle, will decay in a detectable manner within this region, and to evaluate the energy of the photon which enters the collimation system.

(g) Finally, the spectral efficiency of the telescope enters to complete the calculation.

This process of computation was coded for an IBM 650 data-processing machine, and the predictions of various assumptions of energy and angle dependence of the production process were investigated.

B. Predominance of θ_1^0 Detection

The spectral-efficiency curve for the photon counting system (see Fig. 4) indicates that high energies are strongly favored in detection. The counter threshold is 40 Mev, and at the proper energy of a π^0-decay photon (67 Mev) the efficiency is only about 2%. Photons whose energies have been Doppler-shifted upward by virtue of emission from π^0's moving rapidly toward the detector, however, may be counted with efficiencies which rise to over 40%.

The large Q value associated with the two-π^0 mode of the θ_1^0 decay ($\sim$219 Mev), and the high velocities available to the θ_1^0 itself in the 3-body final state, provide the possibility of strong Doppler shifts of photons from this source. The fact that four photons arise from each such decay is of course favorable.

For these reasons we find that the efficiency for observing the θ^0 particles is much greater than for the Λ^0's. The longer lifetime of the K^+ meson and the fact

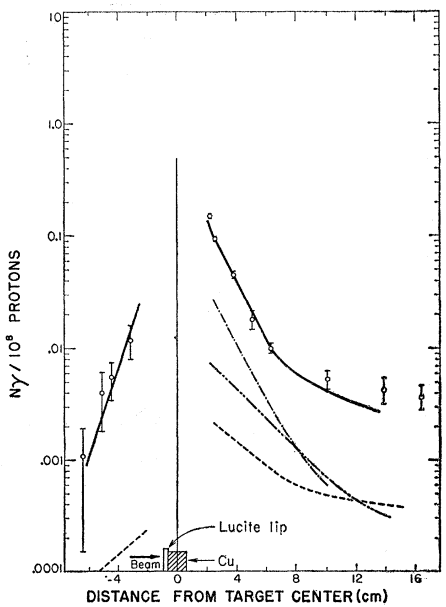

FIG. 11. Calculated curves for θ^0 decay, θ^+ decay, Λ^0 decay, and Σ^+ decay, as compared with the data of Fig. 7. The θ^0 curve is calculated for $|H|^2 \propto 1+6.5\times10^{-3}\,(E^2/M^2-1)^4\cos^8\theta$, the curves for θ^+, Λ^0, and Σ^+ for S-wave only ($|H|^2 \propto 1$), where E=total energy of θ^0, $M=M_\theta c^2$. Values assumed for the curves given. θ^0, ——, $\tau_{\theta^0}=1.5\times10^{-10}$ sec, $\sigma=0.31$ mb "S" wave+0.13 mb "G" wave. θ^+, – – – –, $\tau_{\theta^+}=1.2\times10^{-8}$ sec, $\sigma=1.1$ mb "S" wave. Λ^0, —·—, $\tau_{\Lambda^0}=2.77\times10^{-10}$ sec, $\sigma=1.1$ mb "S" wave. Σ^+, ——·——, $\tau_{\Sigma^+}=0.78\times10^{-10}$ sec, $\sigma=0.95$ mb "S" wave.

[11] Block, Harth, and Sternheimer, Phys. Rev. **100**, 324 (1955).

that it yields only one π^0 in its decay cause the relative intensity of photons from it to be also relatively small near the target. Figures 9 and 11 indicate the relative contributions from these particles under certain production assumptions.

C. Energy and Angle Dependences Examined

1. Spherical Symmetry—S-Wave Production

In Fig. 12 are presented the spatial-decay curves calculated under this assumption, normalized to the experimental data at 2.5 cm downstream from the target, for three different assumed lifetimes of the θ_1^0.

The initial downstream slope can be rather well fit by the lifetime of 1.0×10^{-10} sec. But the upstream yield predicted is low by more than an order of magnitude. Also the downstream prediction falls below the observed data beyond 8 or 10 centimeters.

The excitation function for the photon emission seen at 2.5 cm downstream is, however, fairly well satisfied by S-wave production as shown in Fig. 10.

2. The Strongly Peaked Assumption

If we consider the energy dependence and angular dependence to be free parameters to be adjusted independently as desired, a rather respectable fit to the data may be achieved both upstream and downstream as far as the data extend by a matrix element of the form:

$$|H|^2 \propto \left(\frac{E^2}{M^2}-1\right)\cos^{14}\theta.$$

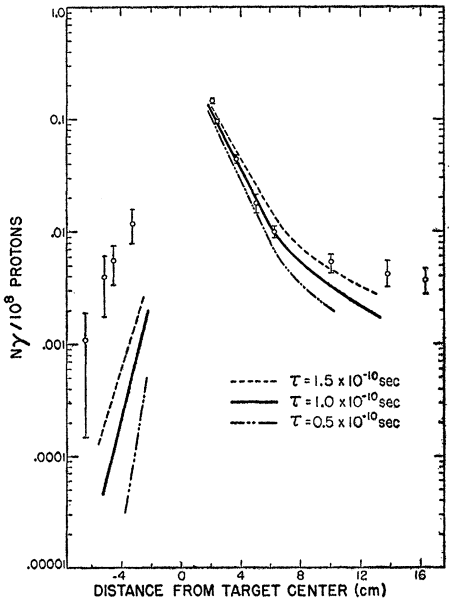

FIG. 12. Comparison of calculated S-wave θ^0 curves (normalized to the experimental data at 2.5 cm) with experimental data for 5.7- to 6.2-Bev protons on a $\frac{1}{2}$-in. Cu target. Several values of mean lifetime are shown; note the poor upstream to downstream agreement with the simple S-wave picture.

This is accomplished, however, at the expense of poor agreement with presently accepted values of the θ_1^0 llfetime. We require about 1.9×10^{-10} sec for this production model. Figure 9 displays the predictions of this model if we assume K^+ mesons and θ^0 mesons are equally produced with this matrix-element form.

The physical basis for such a peaked distribution may be considered in terms of a stripping model investigated by Peaslee for the production reaction.[12] In this case one considers a nucleon as being frequently dissociated into a virtual heavy meson and hyperon state (properly conserving strangeness), and that associated production in a nucleon-nucleon collision takes place via a strong interaction between a virtual pion from one nucleon and a virtual strange particle from the other nucleon. This interaction has been further worked out in terms of a strong K-interaction by Barshay[13] and Schwinger.[14] The stripping picture leads to an effective matrix element with an extreme angular peaking on Peaslee's phenomenological model ($\sim \cos^{30}\theta$), but if this mode of production were mixed with some S-state production, as indicated by the Brookhaven work near threshold, which could also possibly arise from competing 4-body final states, it could reduce to the effective matrix-element fit given above.

The absolute-production cross section of that fraction of θ^0 decay seen by the π^0-decay mode under this assumption is 0.25 ± 0.07 mb.

3. A Mixture of S- and G-Wave Production

Since the energy here employed is considerably above threshold it is likely that several angular-momentum states contribute. Furthermore, other outlet channels than the 3-body final state undoubtedly occur. The calculations of Yujiro *et al.* indicate the relative frequencies of occurrence of 3-, 4-, and 5-body final states predicted by a statistical model with conservation of strangeness and of isotopic spin.[15] Their calculations indicate that the 3-body final state occurs about one-third of the time for 6.2-Bev bombarding proton energy.

A model was therefore attempted which combines a spherically symmetric and a peaked contribution; and the momentum dependence assumed was related to the angular distribution in a manner familiar in wave mechanics. The functional form assumed was

$$|H|^2 \propto 1+a\left(\frac{E^2}{M^2}-1\right)^4\cos^8\theta,$$

with a value of a chosen for best fit to be $a=6.5\times10^{-3}$.

[12] D. C. Peaslee, Phys. Rev. **105**, 1034 (1957).
[13] S. Barshay, Phys. Rev. **104**, 853 (1956).
[14] J. Schwinger, Interactions of the Fundamental Particles, Notes on Lectures by J. Schwinger, Harvard, 1956; prepared by L. S. Rodberg, Massachusetts Institute of Technology (unpublished).
[15] K. Yujiro and K. Keizo, Department of Physics, Osaka University, Osaka, private communication through T. Kotani, 1957.

The result of this choice is shown in Fig. 11, together with spatial-decay curves from other strange particles which could yield photons, with lifetime and cross-section assumptions there stated. The effect of the strong momentum dependence considerably compensates for the weaker angular dependence in the comparison of this result with that of the stripping model, and allows the upstream contribution to be adequate without extreme peaking. The production cross section for θ_1^0's as seen by the π^0-decay mode is, in this case, 0.44 ± 0.10 mb.

VI. SUMMARY

The data allow no precise quantitative conclusions because of the complexity of processes contributing and the experimental and statistical uncertainties. The following qualitative inferences, however, appear to be warranted:

(a) A substantial fraction of the θ_1^0 decay proceeds through the $2\pi^0$ mode. With liberal uncertainty we estimate from our data that the fraction may be near $\frac{1}{4}$. Further elaboration of this experiment is in progress to measure this.

(b) A portion of the θ^0 production involves strong forward-backward peaking in the collision frame of the producing nucleons. It is suggested that high angular-momentum states are prominent, or that a stripping type of reaction may function in the production process.

ACKNOWLEDGMENT

The authors acknowledge with pleasure the cooperation of Dr. E. J. Lofgren, physicist in charge of the Bevatron, and of Mr. Walter Hartsough and Mr. Harry Heard, who were primarily responsible for excellent arrangements and performance of the Bevatron facilities.